Australian Journal of Basic and Applied Sciences, 5(7): 1136-1147, 2011
ISSN 1991-8178

Propose a New Model for Rhyolite Rocks in the East Chah Basheh Mining Region, South Naein (East of Isfahan)

[1]Hossein mirzaee zohreh, [2]Nasr Esfahani Alikhan, [3]Panahpour Ebrahim and [4]Hossein mirzaee zahra

[1]Young researchers club, Khorasgan branch, Islamic Azad University, Isfahan, Iran.
[2]Department of Geology, Islamic Azad University (IAU), Isfahan branch (Khorasgan), Iran.
[3]Departments of Agriculture, Science and Research Branch, Islamic Azad University (IAU), Khouzestan, Iran.
[4]Young researchers club, Khorasgan branch, Islamic Azad University, Isfahan, Iran.

Abstract: The Chah Basheh volcanic rocks are located in the S Naein area, Central Iran, 115 km from east Isfahan. The age of outcrops of rhyolite and tuff rhyolite is Precambrian and contains quartz, albit plagioclase, k-feldspar and opaque. This volcanic rock has a felsophyric texture with SiO2 and k-feldspar. Petrological, mineralogical study and geochemical investigations suggest that the Chah Basheh rhyolite belong to high-k calc-alkaline serie and metaluminous. The statistical technique of discriminated analysis shows that this outcrope has characteristics of orogenic granitoids. These rocks related to volcanic arc active continental margin and these results cannot match with the previous research and probably has a younger age. According to the results continental rift model do not match at least for this region and possibly these rocks are younger than Precambrian and belonge to Oligomiocene age should be revised in age of them.

Key words: Chah Basheh, volcanic rocks, rhyolite, calc-alkaline, metaluminous, active continental margin.

INTRODUCTION

Central Iran zone is largest and most complication geological unit and it cover some parts of east Iran (north of Lut block). In this zone Precambrian rocks outcrops only in the eastern parts and includes gneisses, amphibolites, kinds of schist, marble, mygmatite and anatexy granite. Geologically, Naein area located in central Iran zone (7,6,15 and 16). The study area is located in 115 kilometers east of Isfahan and 20 km south of Naein and that geographic location is between 53°15 - 53°30 and 32°15 - 32°35 (Fig. 1). In the south of Nain area, some outcrops exsist with Infracamprian age.

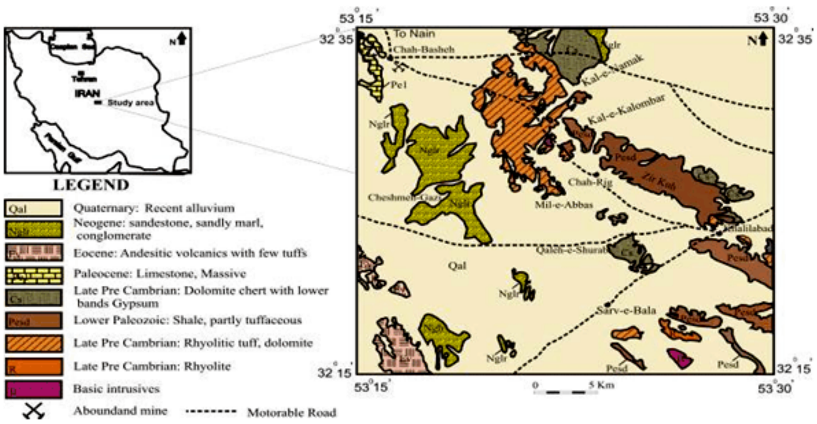

Fig. 1: Geological map of the area (1).

Corresponding Author: Hossein mirzaee zohreh, Member of young research club,Islamic Azad University (IAU), Isfahan branch(Khorasgan), Iran.
E-mail: Zohreh.mirzaee@ymail.com

Oldest rocks of the region belong to Soltanieh geology formation which includes dolomite - rhyolite - shale - limestone with some chert layers. This formation is distinct from other region formations by the fault along Naein - Baft (Dehshir - Baft) (Emami, 1996). Limestone and shale formations are related to the lower Cambrian period containing fossils (Trilobites and Konodont) (vahabi Moghadam, 1993). Outcrops of Infracambrian are reported as the dome and dyke in the south-east of Chah Basheh mine in south Naein. Lithology composition is rhyolite with porphyric texture. Parts of this unit are as tuff (Fig. 1).

Research Methodology:

During the field observations was colected of 60 rock samples from various parts of the study area. After studying the manual sample, 50 thin section preparation and was studied with polarizing microscope. Four samples with XRF method in central lab Isfahan university (Iran) and seven samples with ICP-MS method in ACMELabs Canada was the chemical analysis (Tables 1,2,3). Also, different softwares especially Excel, Minpet and Igpet were used for analysis and drawing charts.

Table 1: Chemical analysis data of the mager oxides with XRF method.

Sample	Unit	11	12	13	14
Rock Type		Rhyolite	Rhyolite	Rhyolite	Rhyolite
SiO_2	%	69.71	74.32	75.23	76.86
Al_2O_3	%	12	11.9	11.7	10.9
Fe_2O_3T	%	0.98	2	1.23	1.13
FeO	%	0.38	0.75	0.47	0.42
Fe_2O_3	%	0.56	1.16	0.71	0.66
CaO	%	4.34	0.71	1.59	0.38
MgO	%	0.28	0.19	0.17	0.09
Na_2O	%	0.18	0.64	0.16	0.21
K_2O	%	9.09	8.44	8.63	8.6
Cr_2O_3	%	0.025	0.048	0.026	0.030
TiO_2	%	0.15	0.12	0.14	0.13
MnO	%	0.046	-	0.045	0.04
SrO	%	0.005	0.008	0.007	-
BaO	%	0.072	0.066	0.059	0.067
LOI	%	2.94	0.95	0.81	1.33
Total	%	99.93	99.97	99.98	99.93
Mg≠		36.14	15.96	21.60	13.70
ACNK		0.53	0.82	0.74	0.83
FM		0.67	0.86	0.81	0.88
MALI		4.93	8.38	7.2	8.43
K_2O/Na_2O		50.71	13.19	53.94	40.95
6		3.22	2.63	2.39	2.2

Table 2: Chemical analysis data of the main oxides with ICP-MS method.

Sample	Unite	1	2	3	4	5	6	7	8	9	10
Rock Type		Diorite	Diorite	Rhyolite	Diorite	Rhyolite	Rhyolite	Rhyolite	Rhyolite	Rhyolite	Rhyolite
SiO_2	%	52.94	49.42	75.39	54.56	73.65	75	69.14	74.88	74.56	69.23
Al_2O_3	%	15.78	15.35	9.58	15.48	10.49	8.09	11	8.98	8.96	13.34
Fe_2O_3T	%	11.84	12.44	5.08	11.02	1.02	1.22	2.89	1.39	1.17	3.79
FeO	%	6.56	7.06	2.16	6.03	0.38	0.51	1.3	0.56	0.47	1.46
Fe_2O_3	%	4.55	4.60	2.67	4.32	0.59	0.65	1.44	0.77	0.65	2.16
CaO	%	4.58	7.14	0.08	4.51	3.02	1.55	1.06	1.16	0.27	0.7
MgO	%	4.19	4.68	1.48	3.81	0.15	0.08	0.15	0.083	0.05	0.2
Na_2O	%	4.43	3.83	0.39	4.38	0.18	0.11	0.15	0.14	0.2	0.27
K_2O	%	2.2	2.49	5.97	2.46	8.96	6.66	6.2	7.49	7.52	9.26
Cr_2O_3	%	0.007	0.002	0.02	0.003	0.01	0.02	0.01	0.03	0.02	0.03
TiO_2	%	2.72	3.16	0.072	1.99	0.13	0.11	0.43	0.12	0.11	0.23
MnO	%	0.096	0.16	0.015	0.075	0.044	0.02	0.25	0.04	0.035	0.03
P_2O_5	%	0.77	1.03	0.006	0.96	0.025	0.041	0.19	0.023	0.034	0.16
SrO	%	0.04	0.07	0.002	0.04	0.004	0.01	0.03	0.01	0.004	0.01
BaO	%	0.08	0.06	0.03	0.06	0.07	0.06	0.008	0.06	0.07	0.05
LOI	%	1.29	0.18	1.98	0.68	.1.24	6.72	6.98	5.69	6.94	4.62
Total	%	100.83	99.86	100.04	99.92	98.91	99.61	98.43	100	99.84	101
Mg ≠	41.45	42.89	36.75	40.87	22.71	12	9.36	10.67	7.82	9.5	
Eu/ Eu*		0.02	0.01	0.03	0.01	0.03	0.03	0	0.02	0.02	0.03

Table 2: Continue.

(La/ Yb)N	19.18	16.47	7	25.65	6.64	8.79	55.79	8.78	18.63	4.39
(Gd/ Yb)N	4.31	4.38	0.89	5.53	1.2	1.15	7.09	1.24	1.79	1.06
ACNK	0.71	0.56	1.04	0.69	0.54	0.63	0.98	0.68	0.79	0.9
(Nb/Zr)N	2.13	2.36	0.82	2.86	0.88	0.77	4.11	0.81	0.83	0.56
FM	0.62	0.61	0.67	0.63	0.8	0.9	0.92	0.91	0.93	0.92
MALI	2.06	-0.81	6.28	2.34	6.12	5.22	5.29	6.47	7.46	8.84
K_2O/Na_2O	0.5	0.65	15.45	0.56	49.99	58.84	41.33	52.44	36.69	33.69
6	4.43	6.23	1.25	4.05	2.73	1.43	1.54	1.83	1.89	3.47

Table 3: Chemical analysis data of elements with ICP-MS method.

Sample	Unite	1	2	3	4	5	6	7	8	9	10
		Diorite	Diorite	Rhyolite	Diorite	Rhyolite	Rhyolite	Rhyolite	Rhyolite	Rhyolite	Rhyolite
Ag	ppm	52	27	57	45	128	58	46	223	46	68
As	ppm	7.8	6.7	2.1	22.7	16.4	6.2	3.3	4	24.7	3.6
Au	ppm	<0.1	<0.1	<0.1	<0.1	<0.1	<0.1	<0.1	<0.1	<0.1	<0.1
Ba	ppm	724	561	285	519	627	540	74	489	608	415
Be	ppm	2	2	1	2	1	<1	2	1	<1	<1
Bi	ppm	0.04	<0.04	<0.04	0.06	<0.04	0.04	0.07	<0.04	<0.04	0.11
Cd	ppm	0.21	0.26	0.05	0.28	0.22	0.08	0.04	0.09	0.05	0.15
Ce	ppm	107.8	133.8	42	145.4	49.91	44.43	386.9	49.83	94.5	46.6
Co	ppm	41.4	49.3	0.8	30.7	1.5	3.7	6.3	2.5	1.2	1.3
Cr	ppm	49	11	136	20	76	170	87	213	137	194
Cs	ppm	0.6	1.4	0.7	0.9	1	0.6	<0.1	0.8	0.6	0.8
Cu	ppm	31.08	42.8	4.12	29.79	9.49	7.86	7.32	10.49	15.2	9.46
Dy	ppm	7	9.5	1.9	7.8	2.7	1.6	7.1	1.9	2.1	4.2
Er	ppm	2.2	3.3	1.3	2.6	1.9	1.2	2	1.5	1.3	3.1
Eu	ppm	3.1	4	0.3	3.7	0.6	0.4	2.2	0.4	0.7	1.1
Ga	ppm	23.52	25.61	16.59	25.99	17.45	8.83	19.58	9.71	6.85	19.7
Gd	ppm	9.2	13.2	2	11.8	3.3	2.3	16.9	2.8	3.6	4.4
Hf	ppm	5.19	7.3	3.93	5.23	4.44	4	0.86	4.07	4.43	5.92
Ho	ppm	1.1	1.5	0.4	1.3	0.6	0.4	0.9	0.4	0.4	1
La	ppm	48.9	59.3	18.9	65.4	21.9	21.1	159	23.7	44.7	21.7
Li	ppm	20.5	25.2	23.1	21.1	3.4	3.3	5.4	2	2.8	1.9
Rb	ppm	46.5	54.9	102.4	44.9	187.5	109.1	100	123.2	140	202
Sr	ppm	351	547	17	336	37	49	246	44	37	57
Y	ppm	27.8	39.4	10.3	34	16.4	9.7	19.3	12.1	11.2	26.6
Zr	ppm	238	301	109.7	235.7	140	126.6	29.7	134.1	139	213
Nb	ppm	34.34	48.19	6.11	45.67	8.39	6.62	8.28	7.34	7.8	8.01
Th	ppm	5.1	6.4	13.4	6.7	8.8	8.4	11.6	10	12	8.1
Pb	ppm	24.42	20.35	2.47	26.69	31.56	2.5	1.81	4.59	4.73	19.9
Zn	ppm	190.1	239.5	25.1	97.9	15.3	4.8	5.4	9.9	7.6	21.3
Ni	ppm	51.2	44.8	6.2	10.9	7.2	13.3	20.9	15.9	11.1	9.1
V	ppm	159	154	5	93	7	6	64	7	7	18
Ta	ppm	1.9	2.4	0.4	2.2	0.4	0.3	0.5	0.4	0.4	0.4
U	ppm	1	1.3	2.3	1.3	1.9	1.9	1.6	1.9	2.1	2.3
W	ppm	113.7	3.7	73.3	6.3	37.2	37.3	>200	59.6	38.4	>200
Sn	ppm	2.8	3.3	0.9	1.9	3.5	1.2	1.1	1.4	0.9	1.9
Mo	ppm	2.47	2.09	1.33	2.42	1.95	2.86	4.28	3.65	2.44	2.45
Pr	ppm	12.8	16.6	4.8	17.8	6.2	5.2	40.9	5.8	10.6	5.6
Nd	ppm	55.9	71.2	18	72.4	24.5	19.4	165	23.2	41	25
Sc	ppm	10.9	12.4	9.3	7.7	7.8	6.1	20.9	6.5	4.6	9.5
Sm	ppm	10.5	13.4	3.1	13.2	4.2	3.5	26.8	4.1	6.8	4.5

Results:

Petrographically, felsic rocks are ranged rhyolite and composite quartz phenocrystals, albite plagioclase and alkali feldspar. The quartz can be seen in the field as phenocrystal and also microcrystal, quartz crystals are often subhedral to euhedral and they are main rock forming minerals. Large quantities of quartz as large phenocryst with Gulf corrosion can be seen in these rocks. There are around quartz phenocryst, fine quartz and less alkali feldspar crystals. This margin can be caused by a fast rise and sudden decrease pressure on the rhyolite magma (Shelly, 1993) (Fig. 2).

After quartz, plagioclase is the most frequent phenocryst. Plagioclases often have euhedral phenocryst, sodice composition and albite to oligoclase compositions. Most plagioclases are polysentetic twin. In these rocks two generations of plagioclase can be seen.

The first generation have large phenocryst of plagioclase which formed in the deep and the second generation of plagioclase microlites that occurred near the surface are signs that magma is cooling fast and have polysentetic twin (Shelly, 1993). Most plagioclases have been alterated to secondary minerals. Most of them are serisity and some of them is cut and fill by secondary minerals such as chlorite, penin (Mg, Fe, Al) 12 (Si, Al) 8O20 (OH) 16 and calcite (Fig. 3B). Alkaline feldspar finds as fine crystal and is present as phenocryst that its value is low and often is kaolinite (Fig. 3A).

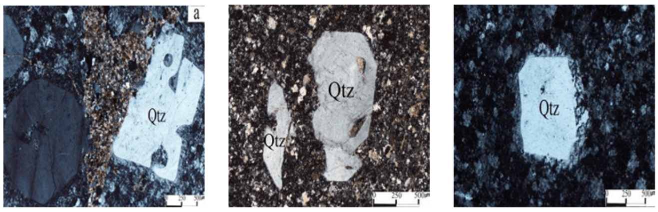

(A) (B) (C)

Fig. 2: A and B- quartz large phenocryst with Gulf corrosion, C) quartz having armor and secondary quartz that calcite and secondary quartz sometimes has been filled rock fractures.

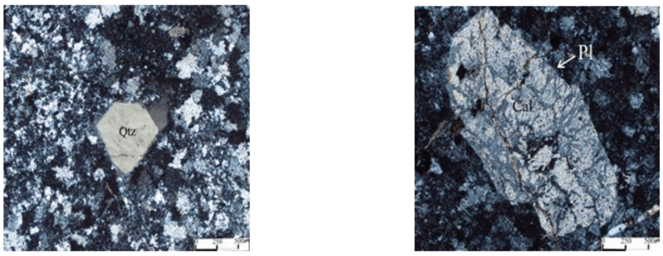

(A) (B)

Fig. 3: A- alkaline feldspar in rocks as small crystals B) plagioclases have been analyzed to secondary minerals.

The minerals opaque can be mentioned as most important minerals in the microscopy sections. The secondary minerals in these sections include serisit, chlorite (more penin type), epidote, calcite (Fig. 4).

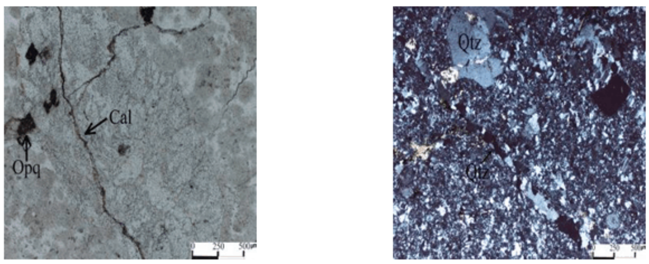

(A) (B)

Fig. 4: A and B- secondary calcite and secondary quartz sometimes are filled rock fractures as veins.

These rocks have diversity in texture but the porphyric texture is the main texture in this rocks and particular texture are felsophyric and glomeroporphyric (Fig. 5).

The main minerals in tuff are plagioclase and quartz that plagioclase is albite. The important secondary minerals include epidote, calcite and opaque minerals. Calcite veins cut microscopy sections. Field is consists of a fine-grained ash tuff that it has been crystallized (Fig. 6).

Average value of the main oxides in the samples is matching with general combining of rhyolite rocks. In this rocks K_2O/Na_2O rate is more than one (13.19 to 58.84, 40.7 average) and it indicate, rhyolite composition is potasic. ACNK molar ratio will change generally around 0.5 to 1 and indicate metaalumyniom. Mg # is with average value of 19.9 (7.8-39).

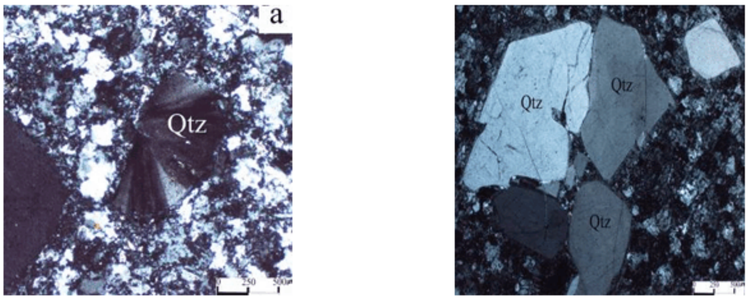

(A) (B)

Fig. 5: A- Felsophyric texture B) Glomeroporphyric texture.

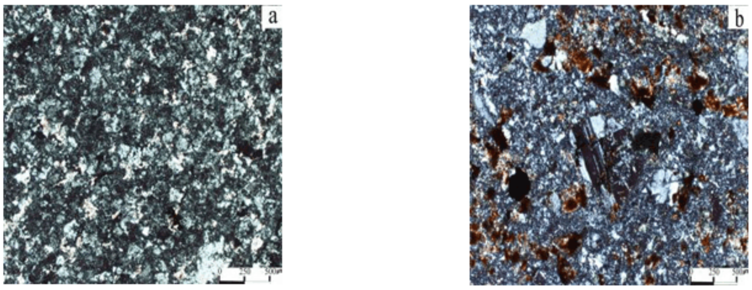

(A) (B)

Fig. 6: Tuff.

One of geochemical classification diagrams for volcanic rocks is oxide - oxide. Cox and colleagues (1979) (Fig. 7A), Le Bas and colleagues (1986) classification volcanic rocks based on Na_2O + K_2O-SiO_2 that were known as the TAS diagram. In this charts, samples placed in the rhyolite range. Winchester and Floyd (1977) have been used the values of rare and minor elements vs. SiO_2 for classification and naming of volcanic rock. In this chart, samples placed in the rhyolite and rhyodasite ranges (Fig. 7B and 7C).

The possibility of alteration and changes in chemical and ore minerals of volcanic igneous rocks are more than internal so Pierce and Kan (1973) were named rocks by using elements that are less displacement (Z, Nb, Y, TiO_2 and Ga). In this chart, samples placed in the rhyolite and rhyodasite region (Fig. 7D).

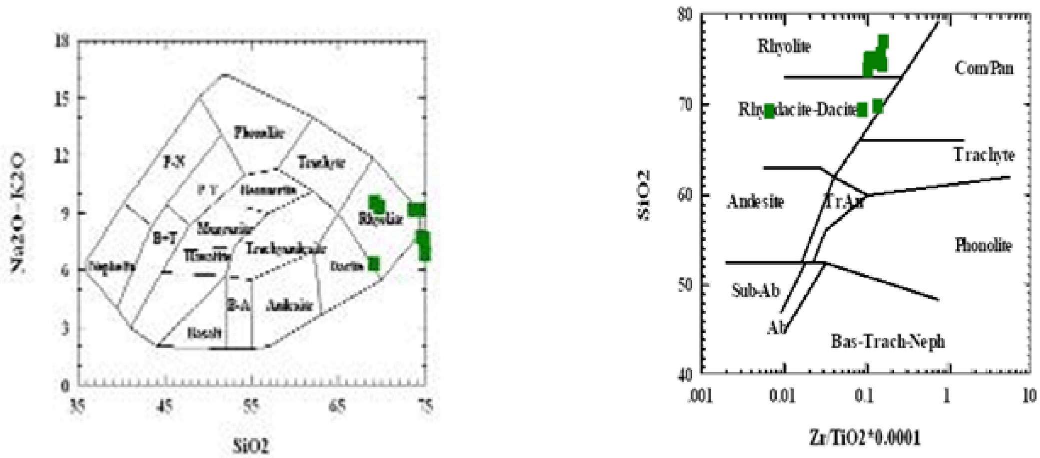

(A) (B)

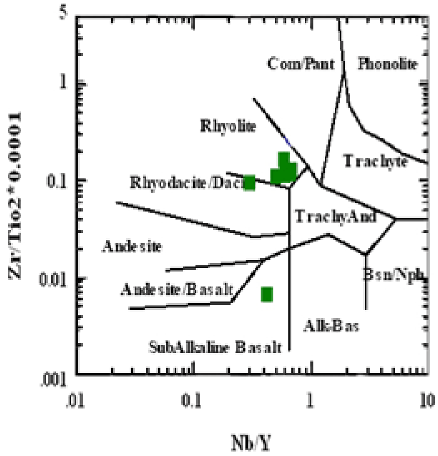

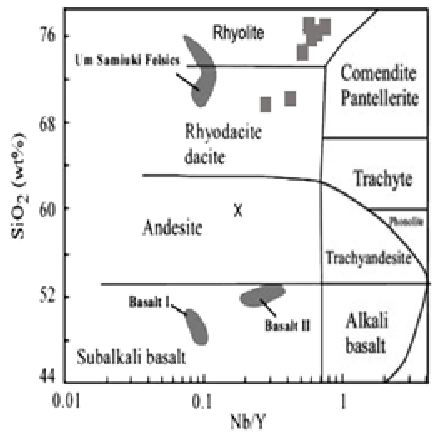

(C) (D)

Fig. 7: A- Cox and colleagues (1979) for volcanic rocks B and C) the Winchester and Floyd (1977) for classification and naming of volcanic rocks D) Pierce and Kan (1973) were named rocks by using elements that move less.

Lemaître and colleagues (1989) were proposed total alkali vs. silica diagrams for separation alkali rock series from sub-alkaline (Fig. 8A). Samples of region is showing semi-alkaline or sub-alkaline afiliatly. Diagram of AFM (10) was used to determine the process of igneous series and for separation calc-alkalin magmas from tholeiitique. Samples show calc-alkalin properties (Fig. 8B). Rahman (1988) can offer figure Na2O + K2O-CaO vs. silica. Samples of rhyolite from the south Naein shows that volcanic rocks are calcic - alkali type on this diagram (Fig. 8C).

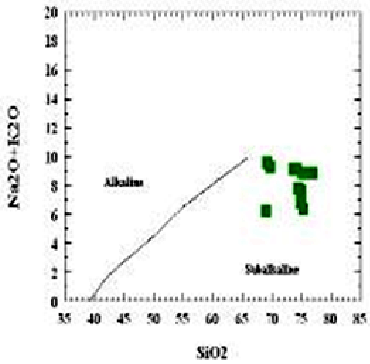

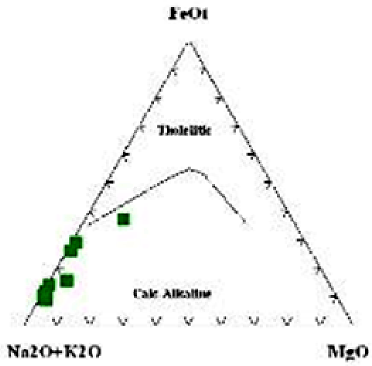

(A) (B)

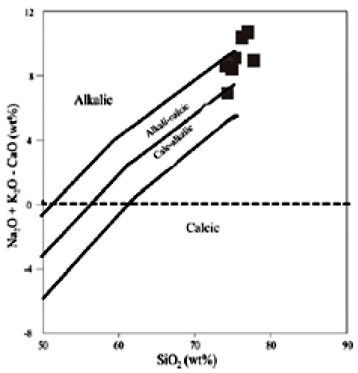

(C)

Fig. 8: A- the alkali vs. silica (Le Maitre, 1989), for separation sub-alkaline and alkaline series, B) AFM diagram in which calc-alkaline series are separated from tholeiitique (10), C) the Na_2O + K_2O-CaO vs. SiO_2 (Rahman, 1988).

In Middlemost diagrams (1985) rhyolite samples (Fig. 9A and B) are located in the range of high-potassium rocks to ultra potassic. rhyolite rocks are potasic series in An-Ab-Or (10) (Fig. 9C).

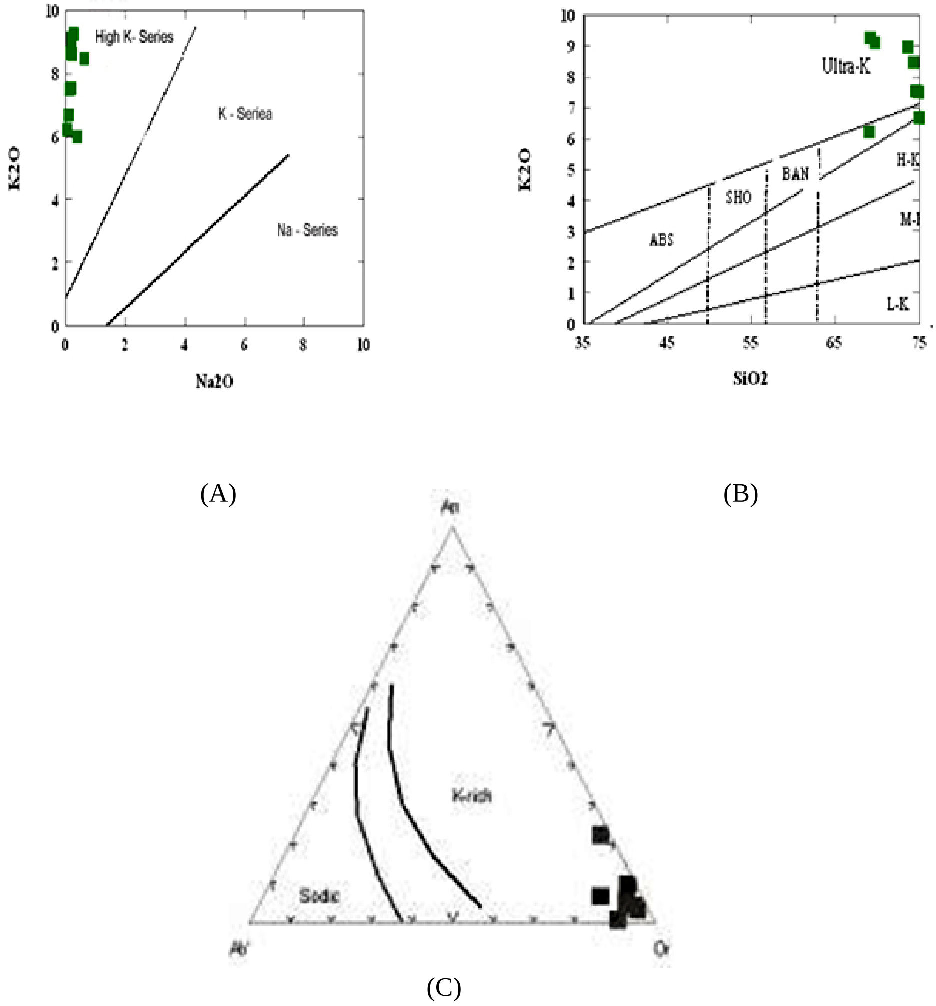

Fig. 9: A and B- The determination of potassium (13) C) The An-Ab-Or (10).

Spider diagrams have been normalized with primary mantle, conderite and N-MORB and interpreted the process of magma formation (Fig. 10). All spider diagrams show that, light rare-earth elements to heavy rare-earth elements generally show rich disruption a lot (except Eu), this mode also applies LILE compared to HFSE (Fig. 10 A and B). Anomaly negative elements Cs, Pb, Sr, Li and Ni than normal conderite well are seen in the samples (Fig. 10C and D).

Spider diagrams that normalized with N-MORB, LREE is riched and HREE is poor. (Fig. 10e and f). Of course, negative anomaly of Eu is observed, In addition, the elements Cs, Ce, Ba, Rb, U, Th, Pb is enriched between 10 and 100 times. Usually rocks of continental crust than MORB are poor from HREE. Than conderite elements, Rb, Ba, Th, U (LILE) show enrichment. Instead, a disability down to Sr, Pb and Li can be seen. This mode indicates the source of contamination with crust. Also, Cs, Cr and Zn have a disability element and elements Ce and Zr are enriched.

The elements Cs, Ba, Rb, Th, U and Pb show enrichment than the primary mantle, but Li disruption is poor and elements Ce and Zr are enriched. Sr and Ni also have the disability. Enrichments of LILE (Cs, Ba, Rb) is due to high mobility of fluid phase act in the subduction zone.

These elements concentration on continental crust and can be offered origin of crustal contamination. Samples to indicate conderite are enriched LREE than HREE. Although this trend shows a poor toward Eu that is characteristic of rhyolite. Amount of Eu / Eu * is average of 0.023 in the samples which is change between 0.034 to 0.003.

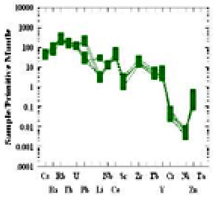

A) Trace elements that have been normalized than the primary mantle.

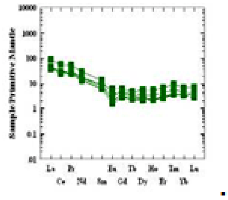

B) Rare earth elements that have been normalized than the primary mantle.

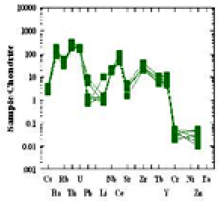

C) Trace elements that have been normalized than the conderite.

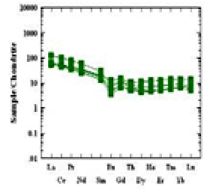

D) Rare earth elements that have been normalized than the conderite.

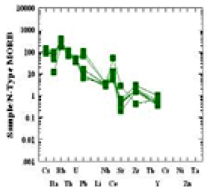

E) Trace elements that have been normalized than the N-MORB.

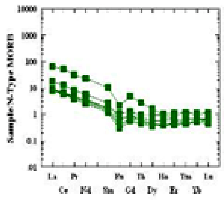

F) Rare earth elements that have been normalized than the N-MORB

Fig. 10: Spider- diagrams.

To determine the tectonomagmatic of rhyolite, a variety of diagrams are proposed with researchers. One of the most common tectenomagmaee diagrams is provided by Pierce and colleagues (1984). In these diagrams, sample type is not between oceanic ridges (ORG) and within plate (WPG), and their show features volcanic arc (VAG) (Fig. 11). However, the high Rb in the samples due to the large role of crust in producing the original magma.

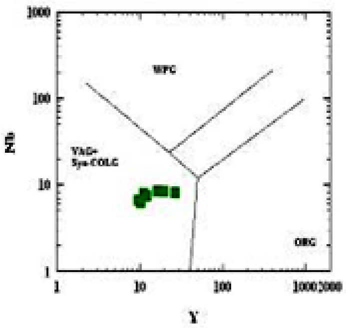

(A)

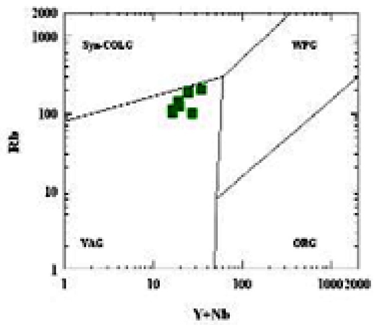

(B)

Fig. 11: To determine the tectonomagmatic of rhyolite magmas (18) based on Nb-Y (A) Based on Rb-Yb (B).

Harris and colleagues (1986) can be classified granitoid magmas in terms of the tectonic environment by using minor elements. In these diagrams the samples located in an active continental margin and thus the ocean subduction slabe is below the continental slabe (VA) (Fig. 12).

(A) (B)

Fig. 12: To determine the tectonomagmatic of granite magmas (9) based on Hf-Rb/10-Ta × 3 (A) and Hf-Rb/30-Ta × 3 (B).

Schandl and Gorton (2002) studied samples; they are in the range of active continental margin (ACM) (Fig. 13A). Brown and colleagues (1984) benefited diagrams Rb / Zr vs. Nb for distinguish various arc volcanic active, in this diagram rhyolite rocks are within the continental arc (Fig. 13B). Studied samples in diagram La / Yb vs. Th / Yb (3) are located in the range of active continental arc (Fig. 13C).

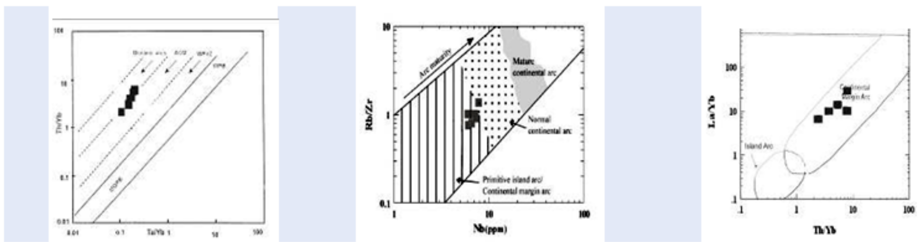

Fig. 13: Diagrams set up the environment: A) logarithmic ratio of Th / Yb against the logarithmic ratio of Ta/Y (23). Studied samples are associated with subduction and are in the range of active continental margins. WPB: within-plate basalts, ACM: active continental margin and WPVZ: volcanic areas within a plate. B) Diagram of Rb / Zr versus Nb (2). C) Chart La / Yb vs. Th / Yb (3).

Partial melting and crustal contamination are considered as the most important processes of magma.

1. Partial Melting:

Although fractional crystallization is main mechanisms evolved magmas, but only with this process cannot be distinguished the abundance of elements such as aluminium, calcium and sodium of magma, so you can understand the different making processes involved in rhyolite magmas. A process affecting in rhyolite magma the southern part of Naein is partial melting (Fig. 14).

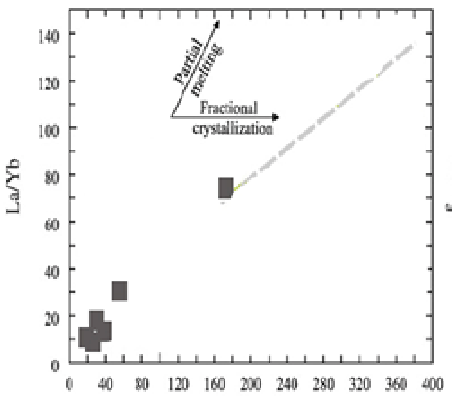

Fig. 14: La/Yb-La diagram (Turner, 1996; Wang, 2008).

2. Crustal Contamination:

Th and La of south Naein rocks is placed within the upper continental crust (Fig. 15), it sign the high contamination of these rocks with continental crust or represent the rhyolite magma originated from the upper crust.

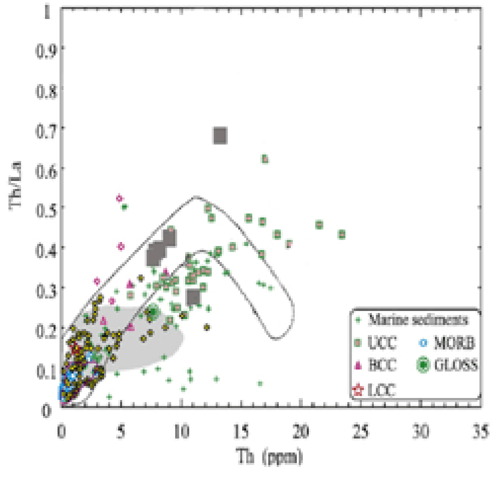

Fig. 15: Th / La-Th diagram (Condie, 1993; Plank, 2005).

Bcc: Bulk continental crust.
LCC: Lower continental crust.
UCC: upper continental crust.
Gloss: Global subducting sediment

***Conclusion*:**

Felsic volcanic rocks in mineralogy and geochemical features are classified in rhyolite groups in the study area. There are Gulf corrosion in quartz, resorption quartz and plagioclase corrosion in all cases that indicate a chemical imbalance and rising magma and rapid reduction in pressure and rose to the role of continental crust or magma mixing (21). Felsic rocks of sub-alkaline geochemical nature are calc-alkaline. Rocks studied in terms of LREE and LILE elements shows many enriched. Wilson (1989) believes rhyolite in the subduction regions are sub-alkaline. High potassium (K> 4 %wt), being rich in iron (FeO / MgO> 3.1) and silica is the symptoms of subduction rocks. Characteristics of subduction zone are rich from elements of K, Rb, Ba and LREE enriched than HREE and HFSE (22). Nb less than 70 ppm is associated with subduction zones (8). Enriched in incompatible elements in felsic volcanic rocks can be explained with influence and important role of crust.

Characterized by high potassium in the rocks may be due to increased levels of crust contamination in the active continental margin magmas (29). In the active continental margin environments there is a relationship between potassium increases with increasing depth of benif page (14). Researchers because of the increased thickness of continental crust and increase its impact at the primary magma knows (23).

Tectonomagmatic diagrams (separation of different tectonic environments) such as rift region, active margins, volcanic arc and continental - continental collision zones are confirmation of an active continental margin environment. Considering the work done, diagram represent subduction rule. This evidence with tectonic models for Precambrian outcrops and central Iran have been inconsistent so perhaps this rhyolite outcrops has a younger age than the age for which they were intended. The role of interactions of a crust is very important in the formation of acid magma causing felsic domes.

According to the results: 1. Continental rift model is not acceptable for this area. 2 - Probably this rocks are younger than Precambrian. 3. Probably these rocks have changed under process metasomatism and changing composition from alkaline nature to calc-alkaline.

REFERENCES

Amidi, S.M., Alavi Tehrani, M.H Nabavi, 1979. The Earth Science maps 1:250,000 of South Naein, Geological Science Publications.

Brown, G.C., R.S. Thorpe, P.C. Webb, 1984. The geochemical characteristics of granitoids in contrasting arcs and comments on magma sources. Journal of Geological Society London, 141: 413-426.

Condie, K.C., 1989. Geochemical changes in basalts and andesites across the Archean-Proterozoic boundary: identification and significance. Lithos 23: 1-18.

Condie, K.C., 1993. Chemical composition and evolution of the upper continental crust:contrasting results from surface samples and shales. Geol., 104: 1-37.

Cox, K.G., J.D. Bell, R.J. Pankhurst, 1979. The interpretation of igneous rocks.George Allen and Unwin., pp: 450.

Davoudzaddeh, M., K. Schmidt, 1983. A review of the Mesozoic paleogeography and paleotectonic evolution of Iran, Geodynamic project (Geotraverse) in Iran. Final report. Geol. Surv. Iran, 51: 474-489.

Emami, M.H, 1996. Magmatism in Iran, Geological Exploration and Mining Geology country.

Green, N.L., 2006. Influence of slab thermal structure on basalt source regions and melting conditions. Lithos, 87: 23-49.

Harris, N.B.W., J.A. Pearce, A.G. Tindle, 1986. Geochemical characteristics of collision-zone magmatism. In: Coward, M.P. and Reis A.C. (eds.), Collision Tectonics. Geol. Society London, 19: 67-81.

Irvine, T.N., W.R.A. Baragar, 1971. A guide to the chemical classification of the common volcanic rocks. Canadian J Earth Science, 8: 523-548.

Le Bas, M.J., Le R.W. Maitre, A. Streckeisen, B.A. Zannetin, 1986. Chemical classification of volcanic rocks based on the total alkali- silica diagram. Journal. Petrol, 27: 745-750.

Le Maitre, R.W., P. Batman, A. Dudek, J. Keller, Lameyre, Le M.J. Bas, P.A. Sabine, R. Scmid, H. Sorensen, A. Streckeisen, A.R. Wooley, B. Zanettin, 1989. A classification of igneous rocks and glossary of terms. Blackwell, Oxford pp: 195.

Middlemost, E.A.K., 1985. Magmas and magmatic rocks. Longman, London.

Miskovic, A., D. Francis, 2006. Interaction between mantle - derived and crustal calc-alkaline magmas in the petrogenesis alkaline of the Sifton Range. Lithos, 87: 204-134.

Nabavi, M.H., 1976. A preface to the Geological Studies of Iran, Geological Science Publications, pp: 440.

Nogole-Sadate, M.A.A., 1985. Les zone de decrochemment ET les vigration structurales en Iran, Conseuences des results de analyze structural de la region de Qom. Geol. Surv. Iran, Rep., 55: 189.

Pearce, J.A., J.R. Cann, 1973. Tectonic setting of basic volcanic rocks determined using trace element analysis. Earth Planet, Sci. Lett, 19: 290-300.

Pearce, J.A., N.B.W. Harris, A.G. Tindle, 1984. Trace element discrimination diagrams for the tectonic interpretation of granitic rocks. Geol. Soc. Spec, Publ, 7: 14-24.

Plank, T., 2005. Constraints from thorium/lanthanium on sediment recycling at subduction zones and the evolution of the continents. J. Petrol, 46(5): 921-944.

Rahman, A., S.J. Ekwere, M. Azmatullah, E. Ukpong, 1988. Petrology and geochemistry of granitic intrusive rocks from the western part of Oban Massif, Southeastern Nigeria [J]. J. African Earth Sciences, 7: 149-157.

Raymond, L.A., 2002. The study of Igneous Sedimentary and Metamorphic Rocks: McGraw Hill, pp: 720.

Sajana, F.G., R.C. Maury, H. Bellon, J. Cotton and M. Defant, 1996. High field strength elements of Pliocene-Pleistocene island-arc basalts Zamboanga Peninsula,Western Mindanao (Philippines). Journal of petrology, 37: 693-726.

Schandl, E.S., M.P. Gorton, 2002. Appplication of high field strength elements to discriminate tectonic setting in VMS environments. Economic Geology, 97: 629-642.

Shelly, D., 1993. Microscopic study of Igneous and Metamorphic rock. Champan and Hall, London, pp: 184.

Shelly, D., 1993. Igneous and metamorphic rocks under the microscope. Chapman and Hall, London, pp: 630.

Turner, S., N. Arnaud, J. Liu, N. Rogers, C. Hawkesworth, N. Harris, S. Kelley, Van P. Calsteren, W. Deng, 1996. Post-collision, shoshonitic volcanism on the Tibetan Plateau: implications for convective thinning of the lithosphere and the source of ocean island basalts. J. Petrol, 37: 45-71.

Vahabi Moghadam, B., 1993. Petrology and petrographic study of metamorphic magmatic rocks, South Naein, MA Petrology, Tehran University.

Wang, Q., A. Derek, Xu. Jifeng, M. Paulo, N. Vasconcelos, W. Yusheng, L. Chaofeng, Y. Yuanshan, Zhu. Tongxing, Zi. Feng, Chu. Zhuyin, 2008. Eocene melting of subducting continental crust and early uplifting of central Tibet Evidence from central-western Qiangtang high-K calc-alkaline andesites, dacites and rhyolites. Earth and Planetary Science Letters. 272.

Wilson, M., 1989. Igneous petrogenesis. Unwin Hyman London, pp: 466.

Winchester, J.A., P.A. Floyd, 1977. Geochemical discrimination of different magma series and their differentiation products using immobile elements.